ESET/SETDB1 gene expression and histone H3 (K9) trimethylation in Huntington's disease

Hoon Ryu*†‡, Junghee Lee*†, Sean W. Hagerty*†, Byoung Yul Soh*†, Sara E. McAlpin*†, Kerry A. Cormier*, Karen M. Smith*†, and Robert J. Ferrante*†‡§¶

*Geriatric Research Education and Clinical Center, Bedford Veteran's Affairs Medical Center, Bedford, MA 01730; and Departments of †Neurology, §Pathology, and ¶Psychiatry, Boston University School of Medicine, Boston, MA 02118

Edited by Mark T. Groudine, Fred Hutchinson Cancer Research Center, Seattle, WA, and approved October 19, 2006 (received for review July 26, 2006)

Chromatin remodeling and transcription regulation are tightly controlled under physiological conditions. It has been suggested that altered chromatin modulation and transcription dysfunction may play a role in the pathogenesis of Huntington's disease (HD). Increased histone methylation, a well established mechanism of gene silencing, results in transcriptional repression. ERG-associated protein with SET domain (ESET), a histone H3 (K9) methyltransferase, mediates histone methylation. We show that ESET expression is markedly increased in HD patients and in transgenic R6/2 HD mice. Similarly, the protein level of trimethylated histone H3 (K9) was also elevated in HD patients and in R6/2 mice. We further demonstrate that both specificity protein 1 (Sp1) and specificity protein 3 (Sp3) act as transcriptional activators of the ESET promoter in neurons and that mithramycin, a clinically approved guanosine–cytosine-rich DNA binding antitumor antibiotic, interferes with the DNA binding of these Sp family transcription factors, suppressing basal ESET promoter activity in a dose dependent manner. The combined pharmacological treatment with mithramycin and cystamine down-regulates ESET gene expression and reduces hypertrimethylation of histone H3 (K9). This polytherapy significantly ameliorated the behavioral and neuropathological phenotype in the R6/2 mice and extended survival over 40%, well beyond any existing reported treatment in HD mice. Our data suggest that modulation of gene silencing mechanisms, through regulation of the ESET gene is important to neuronal survival and, as such, may be a promising treatment in HD patients.

Huntington's disease (HD) is an autosomal-dominant inherited neurological disorder caused by expanded stretches of CAG repeats coding for glutamine in the *Huntingtin* (*Htt*) gene. Polyglutamine [poly(Q)] expansions of mutant Htt (mtHtt) protein lead to a number of cellular abnormalities that include altered nucleosome dynamics and subsequent transcriptional dysregulation (1–4). Consistent with transcriptional repression playing a role in the pathogenesis of HD, decreased acetylation and increased methylation of histones, well established mechanisms of gene activation and silencing, have been found in HD experimental models (5–8). Histone acetylation is involved in the regulation of gene expression and is regulated by the opposing activities of histone acetyltransferases and histone deacetylases (HDACs) (9). The poly(Q) stretches in mtHtt interact physically with CREB binding protein (CBP), a transcriptional coactivator, and block intrinsic CBP histone acetyltransferase activity (2, 5). These specific interactions have led to a model in which mtHtt, by harboring extra glutamines, becomes a hyperactive glutamine-containing corepressor (10). Transcriptional repression may also be attributable to epigenetic modifications, such as histone methylation and histone deacetylation (11). Thus, transcriptional dysfunction has been proposed to play an important role in the neuronal cell death of HD and has been identified as a therapeutic target (12).

We have previously reported that HDAC inhibitors, which act to suppress HDACs and enhance transcription locally, can ameliorate the behavioral symptoms and pathology in models of HD and have provided the rationale for ongoing safety and tolerability clinical trials of HDAC inhibitors in HD patients (6–8). Mithramycin, a clinically approved guanosine–cytosine-rich DNA binding antitumor antibiotic, is one such agent and has resulted in the greatest efficacy to date in HD mice (7). In addition, cystamine, an aminothiol molecule, may also affect transcriptional dysfunction in HD through its ability to cause zinc ejection from transcription regulating zinc finger proteins (13, 14) and secondarily by reducing sequestered transcription factors in insoluble huntingtin aggregates (14). Unfortunately, the mechanisms of altered histone methylation and histone methyltransferase (HMT), which may be key to achieving a greater understanding of the transcription-induced neuronal death, have not been fully investigated (6–7, 15–17).

ERG-associated protein with SET domain (ESET), a novel histone H3 (K9) methyltransferase, has been shown to mediate histone methylation (18). ESET contains both tudor and methyl-CpG binding domains that converge transcription and RNA processing factors, as well as acting as a signature motif for proteins regulating methylated DNA silencing. ESET interacts with a number of enzymes and transcription factors that include HDAC1 and -2, mSin3A and -3B, HP1, and MBD1 (19–21). As such, ESET may be involved in the epigenetic silencing of neuronal genes through its HMT activity (22). Recent reports show that ESET proteins are essential for early development and are associated with gene silencing in human cancers (22, 23).

In the current study, we investigated the association of ESET and histone H3 (K9) trimethylation in the pathogenesis of HD and the biological effects of a polytherapeutic preclinical trial in preventing hypertrimethylation of histone H3 (Lys-9) in R6/2 transgenic HD mice. We show that ESET expression is markedly increased in HD patients and in transgenic R6/2 HD mice and that down-regulation of the ESET promoter results in salubrious effects. Our results suggest that modulation of histone trimethylation and HMT gene expression, through the regulation of ESET, underlies neuroprotective effects in HD mice and, as such, therapeutic approaches targeting dysfunctional histone modification and transcription may provide a rationale in the design of human clinical trials.

Results

Trimethylated Histone (TMH)-H3 (K9) and ESET/SETDB1 Levels Are Altered in HD Brain. To determine whether altered gene silencing is involved in the pathogenesis of HD, we first assessed the level of TMH-H3 (K9) and ESET/SETDB1, a histone H3-K9-specific methyltransferase, in the striatum from HD patients and age-matched control patients. Both TMH-H3 (K9) and ESET immu-

Author contributions: H.R. and R.J.F. designed research; H.R., J.L., S.W.H., B.Y.S., S.E.M., K.A.C., K.M.S., and R.J.F. performed research; H.R. contributed new reagents/analytic tools; H.R., J.L., and R.J.F. analyzed data; and H.R. and R.J.F. wrote the paper.

The authors declare no conflict of interest.

This article is a PNAS direct submission.

Abbreviations: HD, Huntington's disease; HDAC, histone deacetylase; HMT, histone methyltransferase; mtHtt, mutant huntingtin; TMH-H3 (K9), trimethylated histone H3 (Lys-9).

‡To whom correspondence may be addressed. E-mail: hoonryu@bu.edu or rjferr@bu.edu.

This article contains supporting information online at www.pnas.org/cgi/content/full/0606373103/DC1.

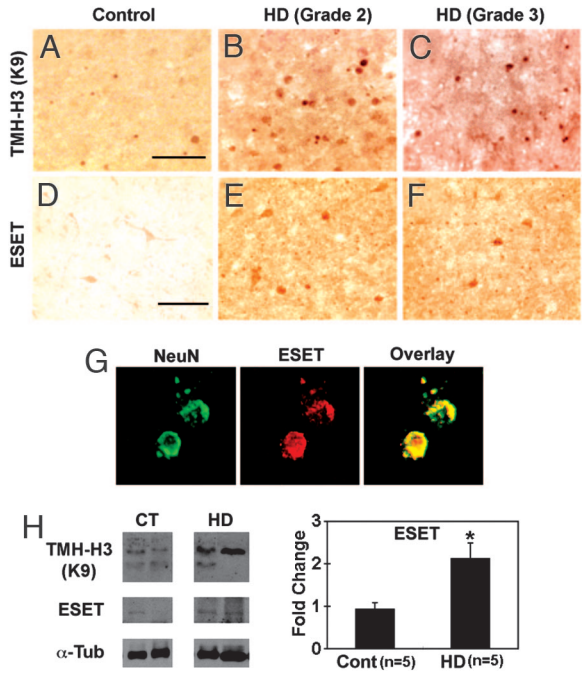

Fig. 1. Increased trimethylation of histone H3 [TMH-H3 (K9)] and altered ESET/SETDB1 expression are found in striatal neurons of HD patients. Immunocytochemical staining for TMH-H3 (K9) (*A–C*) and ESET (*D–F*) is markedly increased in the caudate nucleus of HD grades 2 (*B* and *E*) and 3 (*C* and *F*) brains compared with control brains displaying weak expression of TMH-H3 (K9) (*A*) and ESET (*D*). (Scale bars, 100 μm.) (*G*) Immunoreactivity of ESET is colocalized with NeuN immunoreactivity in caudate neurons in brains from HD patients. (*H*) Western blots show increased TMH-H3 (K9) and ESET protein expression in the caudate tissue from HD patients (*Left*). Densitometric analysis of ESET protein levels in control ($n = 5$) and HD ($n = 5$) (*Right*). *, Significantly different from control at $P < 0.05$.

noreactivity were significantly elevated in both the neocortex and caudate nucleus of grades 2 and 3 HD brains in comparison with age- and postmortem interval-matched control brain samples (Fig. 1 *A–F*). The TMH-H3 (K9) and ESET immunoreactivity was predominantly found in the nucleus of neurons. Double immunofluorescence staining showed the colocalization of ESET with the neuronal marker, NeuN (Fig. 1*G*). Consistent with the immunostaining results, Western blot data showed increased TMH-H3 (K9) and ESET protein levels in the striatal tissue of HD brains (Fig. 1*H*). When normalized to 18S, mRNA levels of ESET were significantly increased ($P < 0.05$) in HD striatal tissue samples by 1.43-fold, in comparison to control brain samples [supporting information (SI) Fig. 6*A*].

Sp3-Dependent Modulation of ESET Promoter Activity and ESET Gene Expression. The murine ESET promoter has been found to have several essential guanosine–cytosine (GC)-rich DNA binding sites for transcription factors such as Sp1 (19). To examine the basal activity and to identify the specific *trans*-element binding site in the ESET promoter, SH-SY5Y cells were transiently transfected with nested-deletion reporter plasmids, including −450/+80, −300/+80, −150/+80, −130/+80, −115/+80, −100/+80, −90/+80, and −10/+80 and a pGL3 basic vector. The transcriptional activity of the −115/+80 ESET reporter was markedly reduced, in which one of the GC-rich sites was eliminated (Fig. 2*A*). To examine the relative contribution of Sp isoforms to the ESET promoter activity, the −130/+80 and −115/+80 ESET reporters were induced by Sp1 and Sp3. The transcriptional activity of the −130/+80 ESET reporter was increased 5-fold by Sp3 and 3-fold by Sp1, but not in the −115/+80 ESET reporter (Fig. 2*B*). This data suggests that both Sp1 and Sp3 act as transcriptional activators of ESET promoters in neurons. The Sp3 levels were increased in R6/2 HD mice (SI Fig. 7*A*). Moreover, siRNA of Sp1 and Sp3 suppressed the basal levels of ESET promoter activity (SI Fig. 7*B*). Our data provides evidence that ESET promoter activity is modulated by GC-rich elements, especially through an Sp3-dependent mechanism. We further characterized the ESET promoter activity by transfecting or cotransfecting Sp1 and Sp3 constructs (SI Fig. 8 *A–C*). Both Sp1 and Sp3 induced ESET promoter activity in a dose-dependent manner (SI Fig. 8*A*). Sp3 showed a stronger induction of ESET promoter activity than Sp1. The combination of Sp1 and Sp3 showed additive effects on the ESET promoter activity (SI Fig. 8 *B* and *C*). The data, herein, support the conclusion that Sp1 and Sp3 are cooperative components in transactivating the ESET promoter.

Mithramycin, a clinically approved anti-tumor antibiotic, binds to DNA interacting with the minor groove with a GC base specificity (24). Mithramycin displaces transcriptional activators that bind to GC-rich binding sites (24) and raises the hypothesis that it may block trimethylation of H3 (K9) in neurons by decreasing expression of the ESET gene. Because transcriptional dysfunction in HD has also been linked to increased histone methylation, we proposed that mithramycin may act to repress transcription by inhibiting the Sp

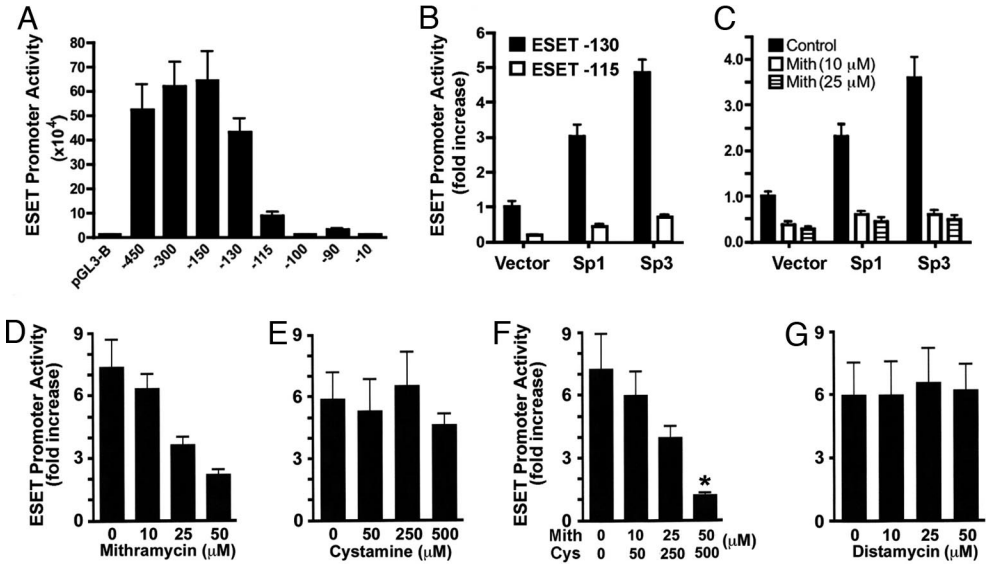

Fig. 2. ESET promoter activity is up-regulated by Sp3 transcription factor and suppressed by mithramycin. (*A*) Mouse ESET promoter activity was determined by using a series of deletion reporter constructs that include Sp binding elements (−450/+80, −300/+80, −150/+80, −130/+80, −115/+80, −100/+80, −90/+80, and −10/+80). (*B*) ESET promoter (−130/+80) activity is up-regulated by Sp3. (*C*) Sp3-induced ESET promoter activity is down-regulated by mithramycin. (*D*) Mithramycin (−150/+80) suppresses basal ESET promoter activity in a dose-dependent manner. (*E*) Cystamine did not suppress ESET promoter activity. (*F*) Combined mithramycin and cystamine inhibited ESET promoter activity. *, Significantly different from 0 dosage at $P < 0.05$. (*G*) Distamycin, an anthracycline analogue, did not suppress ESET promoter activity. The fold change of ESET promoter activity was normalized to pGL3-B vector value (*D–G*). The error bars indicate the SE of three combined experiments.

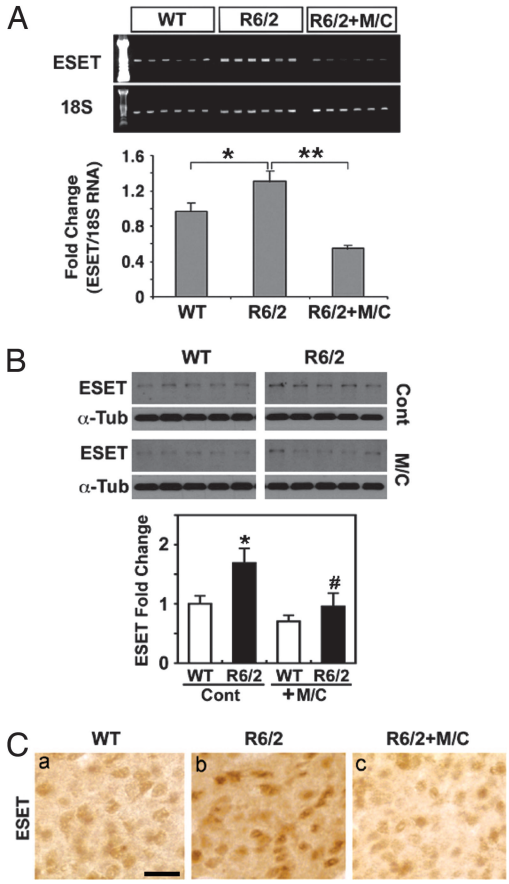

Fig. 3. Pharmacological treatment regulates gene expression and protein levels of ESET/SETDB1 in R6/2 mice. (*A*) Combined mithramycin and cystamine treatment significantly decreased the expression of the ESET gene in R6/2 mice. RT-PCR was performed by using total RNA. The expression level of ESET was normalized to 18S RNA. *, Significantly increased compared with WT at $P < 0.05$; **, significantly decreased compared with vehicle-treated R6/2 mice at $P < 0.01$. (*B*) Combined treatment reduced the protein level of ESET in R6/2 mice. The expression level of ESET was normalized to α-tubulin (α-Tub). *, Significantly increased compared with WT at $P < 0.05$; #, significantly decreased compared with vehicle-treated R6/2 mice at $P < 0.05$. (*C*) ESET immunoreactivity in striatal neurons was markedly increased in R6/2 mice (*b*) compared with WT mice (*a*). The polytherapy attenuated the ESET immunoreactivity (*c*). (Scale bar, 50 μm.)

transcription factors binding to the *cis*-element. To evaluate this possibility, we examined the effect of mithramycin on Sp1- and Sp3-induced ESET promoter activity. Indeed, mithramycin blocked Sp1- and Sp3-induced ESET promoter activity, as well as the basal ESET promoter activity (Fig. 2 *C* and *D*). Cystamine, a known transglutaminase inhibitor and antioxidant that indirectly modulates transcription dysfunction (14), did not influence ESET promoter activity (Fig. 2*E*). Interestingly, however, the combined treatment of cystamine (500 μM) and mithramycin (50 μM) showed a significant additive effect in decreasing ESET promoter activity (Fig. 2*F*). We further investigated whether a constant concentration of cystamine (500 μM) in combination with dose-escalating concentrations of mithramycin may have an affect on ESET transcriptional activity (SI Fig. 9*A*). We found that increasing concentrations of mithramycin, in combination with cystamine resulted in greater down-regulation of ESET transcriptional activity. To test whether alternative DNA binding drugs had a similar neuroprotective effect to mithramycin on ESET promoter activity, we examined distamycin. Distamycin, an anthracycline analog binding the minor groove with adenosine–thymidine base specificity, had no effect on ESET promoter activity (Fig. 2*G*), suggesting that not all DNA binding drugs inhibit ESET gene transcription. In fact, this lack of effect suggests that GC base specificity may be a necessary component of the neuroprotective effects of mithramycin.

Expression of the ESET/SETDB1 Gene Is Modulated by Pharmacological Treatment in R6/2 Mice. We further characterized ESET gene expression in the transgenic R6/2 model of HD to investigate mechanisms that might modulate expression of ESET using therapeutic approaches. ESET gene expression was significantly elevated in R6/2 mice at mid-stage disease (10 weeks). The combined administration of mithramycin and cystamine treatment significantly reduced ESET expression (Fig. 3*A*). ESET mRNA signals at end-stage disease in the R6/2 mice (13 weeks) were only slightly increased, compared with the littermate control mice, and were not significant (SI Fig. 6*B*). These results suggest that ESET mRNA levels may be time-dependently regulated *in vivo* and that up-regulation of ESET mRNA may be an early event in HD pathogenesis. Alternatively, the lower ESET mRNA levels at end-stage disease may be a consequence of significant neuronal death observed in this HD model, in comparison to earlier time points (25).

ESET protein levels were also significantly increased in R6/2 HD mice (70 d) and were subsequently reduced by the combined treatment with mithramycin and cystamine (Fig. 3*B*). Although we found that ESET immunoreactivity was present within both R6/2 and littermate control mouse brains, it was markedly greater in R6/2 mouse brain (Fig. 3*C*). ESET immunoreactivity was present in both the nucleus and cytoplasm of neurons. Combined mithramycin and cystamine treatment reduced ESET immunoreactivity in R6/2 HD mice (Fig. 3*C*).

Combined Treatment with Mithramycin and Cystamine Decreases the Level of TMH-H3 (K9) in R6/2 Mice. Consistent with the finding that there is an up-regulation of ESET in HD patients and HD mice, we observed hypertrimethylation of histone H3 (K9) in tissue sections in the R6/2 mice, in comparison to littermate control mice. There was robust TMH-H3 (K9) immunoreactivity in striatal tissue sections of R6/2 mice, as compared with WT mice. Interestingly, intensely immunostained TMH-H3 (K9)-positive puncta, similar to mtHtt aggregates, were found in R6/2 tissue specimens within neurons and the neuropil (Fig. 4*A*). Further characterization of these structures, by combined immunofluorescence for TMH-H3 (K9) and mtHtt immunoreactivities by confocal microscopy, showed no colocalization of TMH-H3 (K9) immunoreactivity and mtHtt aggregates (Fig. 4*B*). There was, however, a reduction in the size of mtHtt aggregates and intensity of TMH-H3 immunoreactivity. Combined mithramycin and cystamine treatment reduced TMH-H3 (K9) in R6/2 mice to near normal levels (Fig. 4*B*). These findings were confirmed in another HD mouse model. Cystamine also reduced tissue protein levels of TMH-H3 (K9) in N171-Q82 HD mice (SI Fig. 9*B*). Western blot analysis supported the tissue section findings, showing the hypertrimethylation of H3-K9 in R6/2 mice and a significant reduction of ESET protein levels in the combined mithramycin and cystamine-treatment (Fig. 4 *C* and *D*).

Polytherapy with Mithramycin and Cystamine Improves the Clinical and Neuropathological Phenotype in R6/2 Mice. We further demonstrate that the combined treatment with mithramycin and cystamine extended survival, improved body weight and motor performance, and ameliorated the neuropathological sequelae in the R6/2 transgenic HD mice (Fig. 5). Recent findings suggest that the R6/2 HD model exhibits a progressive HD-like phenotype that more closely corresponds to human HD than previously believed (25). There is a clear longitudinal progression of disease along with neuronal death and, as such, recapitulation of the features of HD makes the R6/2 mice highly suitable for preclinical therapeutic trials.

Combined administration of mithramycin and cystamine in the R6/2 mice extended survival over 40%, well beyond any

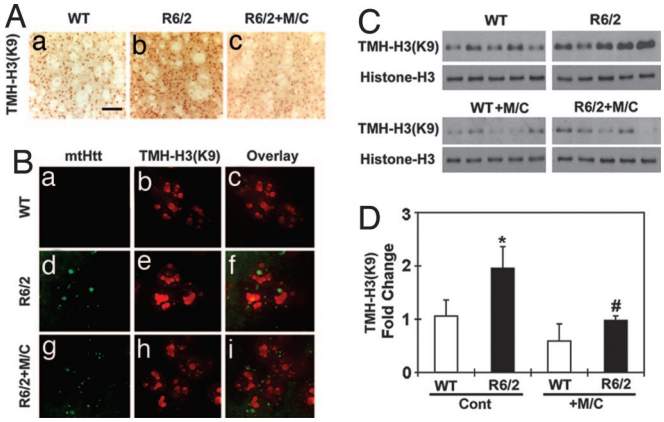

Fig. 4. Pharmacological treatment modulates the level of TMH-H3 (K9) in R6/2 mice. (*A*) The TMH-H3 (K9) immunoreactivity in striatal neurons was markedly increased in R6/2 mice (*b*) compared with WT mice (*a*). Polytherapy attenuated the TMH-H3 (K9) immunoreactivity (*c*). (Magnification, ×10; scale bar, 200 μm.) (*B*) Combined mithramycin and cystamine treatment reduced mtHtt aggregates and sequestration of TMH-H3 (K9) by mtHtt in R6/2 mice. (*a*, *d*, and *g*) MtHtt (green). (*b*, *e*, and *h*) TMH-H3 (K9) (red). (*c*, *f*, and *i*) Overlay images. (*C*) Mithramycin and cystamine combinational treatment significantly reduced the level of TMH-H3 (K9) in R6/2 mice. The level of TMH-H3 (K9) was normalized to total histone H3 level. (*D*) Densitometric analysis of TMH-H3 (K9) protein levels from the data in *C*. *, Significantly increased compared with WT at $P < 0.05$; #, significantly decreased compared with vehicle-treated R6/2 mice at $P < 0.05$.

reported treatment in HD mice. Mithramycin and cystamine treatment alone resulted in a 29% and 20% extension, respectively, in survival and was consistent with previous work, providing context to the current study (untreated R6/2 mice, 99.3 ± 1.4; mithramycin 150 μg/kg, 128.1 ± 5.4 d; cystamine 112 mg/kg, 119.3 ± 3.9 d; combined mithramycin/cystamine treatment, 139.1 ± 6.2 d) (Fig. 5*A*). Significant differences in body weight occurred after 12 weeks as an epiphenomenon of survival extension and not as a primary independent event related to the combined mithramycin and cystamine treatment (Fig. 5*B*). In addition, the combined treatment significantly improved rotarod performance throughout the lifespan of the R6/2 treated-mice from 5 weeks, as compared with untreated R6/2 mice (Fig. 5*C*). The polytherapy regimen delayed gross brain atrophy, ventricular hypertrophy, and striatal neuronal atrophy seen in R6/2 mice such that at 90d of age there was no significant difference in these outcomes compared with WT littermate mice (Fig. 5*D*). In comparison, there was a 20% reduction in brain weight in untreated R6/2 mice compared with treated R6/2 mice and littermate WT mice (untreated R6/2 mice, 356.3 ± 34.4 mg; WT littermate control mice, 450.1 ± 15.9 mg; combined mithramycin/cystamine treatment, 446.7 ± 16.2 mg). Similarly, there was a marked significant difference in neuronal size in untreated R6/2 mice compared with treated R6/2 mice and littermate WT mice (untreated R6/2 mice, 56.9 ± 18.2 mm^2; WT littermate control mice, 33.1 ± 12.1 mm^2; combined mithramycin/cystamine treatment, 31.7 ± 14.3 mm^2). Lastly, combined therapy resulted in significant amelioration of mtHtt aggregates in the neostriatum [Huntingtin aggregates in untreated R6/2 mice, $5.18 \times 10^6 \pm 1.47$; mithramycin/cystamine-treated R6/2 mice, $2.73 \times 10^6 \pm 1.34$; $F(2,20) = 4.35$; $P = 0.01$], likely as a consequence of the cystamine treatment because mithramycin alone does not reduce mtHtt aggregates (7).

Discussion

Chromatin remodeling through histone acetylation and histone methylation ensures DNA transcription. Altered nucleosome dynamics by these complexes may result in transcription dysregulation and subsequent disease expression. Whereas histone acetylation improves transcription, histone methylation is associated with decreased transcription activity. One mechanism of pathogenesis in HD has been linked to global transcriptional repression, such as epigenetic histone modification (1, 7). ESET is a HMT that specifically targets histone-3 at its Lys-9 (H3 K9) site with a trimethyl group (18). Because hyperdimethylation of H3-K9 has been shown in murine models of HD (6–8), a gain of HMT function appears to be linked to the pathogenic gene silencing seen in the disease process. Increasing interest has been focused on molecules such as HDAC inhibitors, which can induce histone hyperacetylation via suppression of HDAC activity. The biological action of HDAC inhibitors is associated with improved neuronal survival in HD (6, 26). Therefore, therapeutic approaches targeting dysfunctional histone modifi-

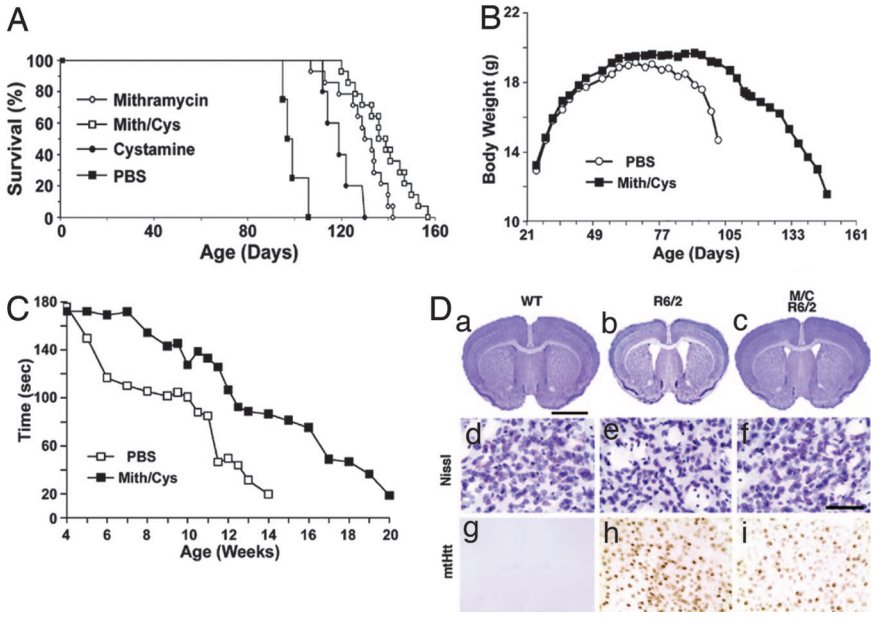

Fig. 5. Combined mithramycin and cystamine treatment extends survival and improves the clinical and neuropathological sequelae in R6/2 mice. (*A*) Kaplan–Meier probability of survival analyses of mithramycin and cystamine alone and combined treatment in R6/2 mice. (*B*) Effects of polytherapy on body weight in R6/2 mice. (*C*) Effects of combined treatment on rotarod performance. The motor performance in R6/2 mice was significantly improved throughout the temporal sequence of the experiment. *, $P < 0.01$. (*D*) Photomicrographs of coronal sections from the rostral neostriatum through the level of the anterior commissure in a WT littermate mouse (*a*), a PBS-treated R6/2 mouse (*b*), and a mithramycin and cystamine-treated R6/2 mouse (*c*) at 90 d. There was gross atrophy of the brain in the PBS-treated R6/2 mouse along with ventricular hypertrophy (*b*) as compared with the WT littermate control mouse (*a*). In contrast, the mithramycin and cystamine-treated R6/2 mouse brain (*c*) showed reduced gross brain atrophy and ventricular enlargement compared with the PBS-treated R6/2 mouse (*b*). Corresponding Nissl-stained tissue sections from the dorsomedial aspect of the neostriatum in a WT littermate control (*d*), PBS-treated R6/2 mouse (*e*), and mithramycin and cystamine-treated R6/2 mouse (*f*) are also shown. There was significantly less neuronal atrophy ($P < 0.01$) in the mithramycin and cystamine-treated R6/2 mouse compared with the PBS-treated R6/2 mouse. Reduction of mtHtt immunoreactivity in the mithramycin and cystamine-treated R6/2 mice (*i*). (Scale bars: *Da*, 2 mm; *Df*, 100 μm.)

cation and transcription may identify novel biological activities and provide a rationale in the design of human clinical trials.

One mechanism of gene silencing involves the methylation of histone H3 at Lys-9 (11). Interestingly, an examination of this histone H3 site in human HD and R6/2 HD mice revealed increased trimethylation of Lys-9 (H3-K9) relative to control specimens. When R6/2 HD mice were treated with combined administration of mithramycin and cystamine, agents that improve transcription, trimethylation of H3-K9 was reduced to the levels seen in WT controls, regulating histone homeostasis. Mithramycin is a well known aureolic acid antibiotic that binds to DNA sequences with guanosine–cytosine (GC) base specificity in the presence of magnesium or zinc, and results in the selective inhibition of DNA-dependent RNA synthesis/gene expression, displacing Sp1 from its GC-rich binding site (27). The results of studies by Miller and colleagues supported the notion that mithramycin may act as an anti-tumor agent by selectively down-regulating genes, such as c-Myc, implicated in dysregulated growth (27). These observations formed the basis for mithramcyin's use in humans as a cancer therapy by Vogelstein and Kinzler (28). Our present data on the modulation of the ESET promoter and gene expression reconcile Sp1 and Sp3 displacement with the neuroprotective ability of mithramycin. It is, therefore, likely that the mechanism of mithramycin action depends on the inhibition of Sp1 and Sp3 transcriptional activity. In fact, this regulatory effect suggests that GC base specificity may be a necessary component of ESET gene regulation by mithramycin.

Cystamine is the disulfide form of the free thiol cysteamine and has had a number of clinical and experimental uses in disease and prevention of cell death (14, 29). While cystamine may have anti-oxidant and anti-apoptotic properties, it is a potent transglutaminase inhibitor and significantly reduces the formation of Htt aggregates and sequestration of transcription factors critical to cell survival (30). Although the pathological significance of cytosolic and nuclear mtHtt aggregation remains unclear, the evidence continues to point to a proximal toxicity residing in mtHtt, its proteolytic fragments, and their interactions with other proteins. Cystamine suppresses Htt protein aggregation and extends survival in HD mice (14). Inhibition of aggregation may be neuroprotective on a number of different levels. These include reducing the mass effect of cellular aggregate burden and the sequestration of critical transcription factors and neuronal proteins that are essential for neuronal survival (14, 31). It has recently been found that the neuroprotective effect of cystamine involves stimulation of the secretory pathway through formation of clathrin-coated vesicles containing brain-derived neurotrophic factor (BDNF) (32). It is also possible that cystamine may act additively with mithramycin by directly increasing the transcription of critical neuroprotective factors in HD (31).

ESET is an ERG-associated protein that functions in transcription regulation and the subsequent modification of local chromatin through the methylation of histones, leading to gene silencing (19, 33). ESET is also involved in maintaining heterochromatin. As a HMT, ESET may form complexes with other chromatin remodeling enzymes in modulating gene transcription (34). We show that ESET expression is markedly increased in HD patients and in R6/2 transgenic HD mice and that ESET specifically methylates and increases the protein level of trimethylated histone H3 (K9), a marker of gene silencing. We also show that both Sp1 and Sp3 act as transcriptional activators of ESET promoters in neurons. Combined pharmacological treatment with mithramycin and cystamine, two transcription modulating agents, down-regulates ESET gene expression and reduces the hypertrimethylation of histone H3 (K9), and significantly ameliorates the behavioral and neuropathological phenotype in R6/2 mice.

These findings suggest that polytherapeutic modulation of gene silencing mechanisms and altered signaling cascades that underlie the HD pathology may be a useful strategy in the treatment of HD.

Materials and Methods

Human Tissue Samples. Samples of striatum and the superior frontal cortex were pathologically verified and graded according to neuropathological criteria (35). All control subjects were free of neurological disease and were matched to the HD cases based on postmortem interval (PMI) and age. Tissue specimens were dissected fresh from six control patients (mean age, 68.5 years; range, 56–72 years) and six patients with HD (two grade 2 cases and four grade 3 cases; mean age, 71.1 years; range, 57–76 years) and were flash frozen in liquid nitrogen (stored in −80°C freezer) with contiguous specimens placed in cold (4°C) 2% paraformaldehyde/lysine/periodate solution. The postmortem intervals from all cases did not exceed 16 h (mean postmortem interval, 11.4 h; range, 4–16 h). Tissue blocks were cryoprotected in increasing concentrations of 10% and 20% glycerol/2% DMSO and serially cut at 50 μm.

Animals. The male R6/2 mice were bred with females from their background strain (B6CBAFI/J), and offspring were genotyped by using PCR. Any mice that had base-paired banding above 550 and below 500, as identified from PCR analysis, were excluded from the study. CAG repeat length remained stable within a 147–153 range. All mice were weighed at 20 d of age and equally distributed according to weight and parentage within each cohort ($n = 10$). Female mice were used in the experimental paradigms. The mice were housed five in each cage under standard conditions with ad libitum access to food and water. All mice were handled under the same conditions by one investigator blinded to the genotype of the mice and the type of diet administered.

Therapeutic Intervention. Using previously reported optimal doses of cystamine (112 mg/kg/d cystamine dihydrochloride given orally in drinking water, 450 mg/liter tap water; Sigma, St. Louis, MO) and mithramycin (150 μg/kg/d mithramycin A, dissolved in PBS, 100-μl i.p. injection; Serva Feinbiochemica, Heidelberg, Germany) (14, 36), we treated cohorts ($n = 10$) WT and R6/2 mice alone or with a combination of cystamine and mithramycin, starting at 28 d. Control groups were treated with PBS injection or untreated.

Clinical Assessment: Motor Performance, Body Weight, and Survival. Motor performance was assessed weekly from 28 to 63 d of age and twice weekly from 63 to 90 d of age in the R6/2 and littermate control mice as reported (6). Body weights were recorded twice weekly at the same day and time of day in all groups. HD mice were euthanized when they were unable to right themselves after being placed on their back and initiate movement after being gently prodded for 30 s. A limited number of deaths occurred overnight and were recorded the following morning. Two independent observers confirmed the criterion for euthanization (R.J.F. and K.M.S.). These procedures were performed in accordance with *Guide for the Care and Use of Laboratory Animals* guidelines and were approved by both the Veterans Administration and Boston University animal care committees.

Histopathology. At 28 d of age, groups ($n = 10$) of R6/2 and littermate WT control mice were placed on either an unsupplemented diet or a diet supplemented with combined cystamine and mithramycin. At 90 d of age, mice were deeply anesthetized and transcardially perfused with 2% buffered paraformaldehyde. Brains were cryoprotected and serially sectioned (50 μm). Both human and mouse tissue sections were stained for Nissl substance and immunostained for Htt immunoreactivity (Htt rabbit polyclonal antibody, EM48; dilution, 1:1,000; Chemicon, Temecula, CA), ESET/SETDB1 (ESET rabbit polyclonal antibody; dilution, 1:200; Upstate Biotechnology, Lake Placid, NY), and trimethylated histone H3 (K9) (rabbit polyclonal antibody; dilution, 1:200; Upstate Biotechnology) by using a previously reported conjugated second antibody method (6). Antibody complexes were visualized

by using diaminobenzidine. Preabsorption with excess target protein, or omission of either primary or secondary antibody, was used to demonstrate antibody specificity and background generated from the detection assay.

Stereology Quantitation. Serial-cut coronal tissue sections from the rostral segment of the neostriatum at the level of the anterior commissure (interaural 5.34 mm, bregma 1.54 mm to interaural 3.7 mm, bregma −0.10 mm) were used for htt aggregate analysis. Unbiased stereological counts of htt-positive aggregates (>1.0 μm) were obtained from the neostriatum in 10 mice each from treated and untreated R6/2 mice at 90 d by using Neurolucida and Stereo Investigator software (MicroBrightField, Colchester, VT). The optical dissector counting method was used in which htt-positive aggregates were counted from serial sections in a defined volume of the neostriatum. Striatal neuron areas were analyzed by microscopic video capture with a Windows-based image analysis system for area measurement (Optimas Bioscan, Edmonds, WA). All computer-identified cell profiles were manually verified as neurons and exported to Excel (Microsoft, Seattle, WA). Cross-sectional areas were analyzed by using StatView (Brain Power, Calabasas, CA).

RT/PCR Analysis. Total RNA was extracted from the neostriatum of human and mouse brain by using the RNeasy Lipid Tissue mini kit (Qiagen, Valencia, CA). RNA was measured in a spectrophotometer at 260-nm absorbance. RNA analysis was conducted as follows. Fifty nanograms of RNA were used as a template for quantitative RT-PCR amplification, using SuperScript One-Step RT-PCR with Platinum *Taq* (Invitrogen, Carlsbad, CA). Primers were standardized in the linear range of cycles before onset of the plateau. The sequence of the primers was as follows: ESET/SETDB1 forward, 5′-ACATCCTCAGCCTCTGCACT-3′; ESET/SETDB1 reverse, 5′-TTCCAGTACCGGTCAGATCC-3′; 18S RNA forward, 5′-CCGAGATTGAGCAATAACAGG-3′; 18S RNA reverse, 5′-AGTTCGACCGTCTTCTCAGG-3′. The conditions of one step RT-PCR for ESET primers were as follows: 30 min at 50°C, 2 min at 94°C, and 35 cycles of amplification for 15 s at 94°C for 15 s, 30 s at 68°C, 1 min at 70°C, and 10 min at 72°C and 4°C. 18S RNA primers were complete at 30 cycles and 55°C for the annealing step. Differences were assessed by using an unpaired, two-tailed Student *t* test.

Acid Extraction of Histone Protein and Histone Methylation Assay. Tissue lysate was obtained by homogenizing minced brain in 500 μl of PBS buffer containing 0.4 mM sodium butyrate, 5% Triton X-100, 3 mM DTT, 1 mM sodium orthovanadate, 5 mM sodium fluoride, 3 mM PMSF, 3 mM DTT, 0.5 μg/ml leupeptin, and 10 μg/ml aprotinin as described (7, 37). Two hundred microliters of the lysate was washed twice with the above described 5% Triton buffer, and histones were extracted by solubilization in 0.2 M HCl. After neutralizing the pH of the acid extracted solution containing the histone pool with ammonium acetate, protein was quantified and separated in SDS/15% PAGE for the Western blot analysis of methylated histone H3 (K9) by using anti-trimethyl-histone H3 (Lys-9) antibody (1:1,000; Upstate Biotechnology).

Western Blot Analysis for ESET/SETDB1. Brain tissue was homogenized in 2.5× volume of 50 mM Tris·HCl/10% glycerol/5 mM magnesium acetate/0.2 mM EDTA/0.5 mM DTT. Protein concentration was determined by using the protein assay kit (Bio-Rad, Hercules, CA). Thirty micrograms of protein was subjected to SDS/10% PAGE and blotted with 1:1,000 diluted anti-ESET/SETDB1 (Upstate Biotechnology). Protein loading was controlled by probing for β-actin (1:2,500; Sigma) or α-tubulin (1:2,500; Sigma) on the same membrane.

ESET/SETDB1 Promoter Activity Analysis. ESET promoter analysis was performed by using a reporter construct containing −435 to +87, including nested deletion constructs, of the 5′ regulatory region of the mouse ESET/SETDB1 gene (38). The SH-SY5Y cells were used in the transient transfection assays and were treated with mithramycin at 10 or 50 μM for the indicated times. Reporter activity assays (at 48 h after transfection) and data analysis were performed (39).

Statistics. The data are expressed as the mean ± SEM. Statistical comparisons of rotarod, weight data, and histology data were compared by ANOVA or repeated-measures ANOVA. Survival data were analyzed by Kaplan–Meier survival curves.

H.R. and R.J.F. are grant awardees of the Jerry McDonald Huntington's Disease Foundation from Boston University School of Medicine. This work was supported by National Institutes of Health Grants NS52724-01 (to H.R.), P30 AG13846 (to J.L.), NS045242 (to R.J.F.), and NS045806 (to R.J.F.); the High Q Foundation (H.R. and R.J.F.); the Huntington's Disease Society of America (H.R. and R.J.F.); and the Veterans Administration (R.J.F.).

1. Cha JH (2000) *Trends Neurosci* 23:387–392.
2. Nucifora FC, Jr, Sasaki M, Peters MF, Huang H, Cooper JK, Yamada M, Takahashi H, Tsuji S, Troncoso J, Dawson VL, *et al.* (2001) *Science* 291:2423–2428.
3. Dunah AW, Jeong H, Griffin A, Kim YM, Standaert DG, Hersch SM, Mouradian MM, Young AB, Tanese N, Krainc D (2002) *Science* 296:2238–2243.
4. Li SH, Cheng AL, Zhou H, Lam S, Rao M, Li H, Li XJ (2002) *Mol Cell Biol* 22:1277–1287.
5. Steffan JS, Bodai L, Pallos J, Poelman M, McCampbell A, Apostol BL, Kazantsev A, Schmidt E, Zhu YZ, Greenwald M (2001) *Nature* 413:739–743.
6. Ferrante RJ, Kubilus JK, Lee J, Ryu H, Beesen A, Zucker B, Smith K, Kowall NW, Ratan RR, Luthi-Carter R, *et al.* (2003) *J Neurosci* 23:9418–9427.
7. Ferrante RJ, Ryu H, Kubilus JK, D'Mello S, Sugars KL, Lee J, Lu P, Smith K, Browne S, Beal MF, *et al.* (2004) *J Neurosci* 24:10335–10342.
8. Gardian G, Browne SE, Choi DK, Klivenyi P, Gregorio J, Kubilus JK, Ryu H, Langley B, Ratan RR, Ferrante RJ, *et al.* (2005) *J Biol Chem* 280:556–563.
9. Marks PA, Richon VM, Miller T, Kelly WK (2004) *Adv Cancer Res* 91:137–168.
10. Freiman RN, Tjian R (2002) *Science* 296:2149–2150.
11. Hake SB, Xiao A, Allis CD (2004) *Br J Cancer* 90:761–769.
12. Rubinsztein DC (2004) *J Biol Chem* 279:4988–4999.
13. McDonnell NB, De Guzman RN, Rice WG, Turpin JA, Summers MF (1997) *J Med Chem* 40:1969–1976.
14. Dedeoglu A, Kubilus JK, Jeitner TM, Matson SA, Bogdanov M, Kowall NW, Matson WR, Cooper AJ, Ratan RR, Beal MF, *et al.* (2002) *J Neurosci* 22:8942–8950.
15. Peters AH, Kubicek S, Mechtler K, O'Sullivan RJ, Derijck AA, Perez-Burgos L, Kohlmaier A, Opravil S, Tachibana M, Shinkai Y, *et al.* (2003) *Mol Cell* 12:1577–1589.
16. Lachner M, O'Sullivan RJ, Jenuwein T (2003) *J Cell Sci* 116:2117–2124.
17. Zhang Y, Reinberg D (2001) *Genes Dev* 15:2343–2360.
18. Rea S, Eisenhaber F, O'Carroll D, Strahl BD, Sun ZW, Schmid M, Opravil S, Mechtler K, Ponting CP, Allis CD, *et al.* (2000) *Nature* 406:593–599.
19. Yang L, Mei Q, Zielinska-Kwiatkowska A, Matsui Y, Blackburn ML, Benedetti D, Krumm AA, Taborsky GJ, Jr, Chansky HA (2003) *Biochem J* 369:651–657.
20. Tamaru H, Zhang X, McMillen D, Singh PB, Nakayama J, Grewal SI, Allis CD, Cheng X, Selker EU (2003) *Nat Genet* 34:75–79.
21. Fuks F (2005) *Curr Opin Genet Dev* 15:490–495.
22. Li H, Rauch T, Chen ZX, Szabo PE, Riggs AD, Pfeifer GP (2006) *J Biol Chem* 281:19489–19500.
23. Dodge JE, Kang YK, Beppu H, Lei H, Li E (2004) *Mol Cell Biol* 24:2478–2486.
24. Jones DE, Jr, Cui DM, Miller DM (1995) *Oncogene* 10:2323–2330.
25. Stack EC, Kubilus JK, Smith K, Cormier K, Del Signore SJ, Guelin E, Ryu H, Hersch SM, Ferrante RJ (2005) *J Comp Neurol* 490:354–370.
26. Ryu H, Lee J, Olofsson BA, Mwidau A, Dedeoglu A, Escudero M, Flemington E, Azizkhan-Clifford J, Ferrante RJ, Ratan RR (2003) *Proc Natl Acad Sci USA* 100:4281–4286.
27. Miller DM, Polansky DA, Thomas SD, Ray R, Campbell VW, Sanchez J, Koller CA (1987) *Am J Med Sci* 294:388–394.
28. Vogelstein B, Kinzler KW (2004) *Nat Med* 10:789–799.
29. Borrell-Pages M, Canals JM, Cordelieres FP, Parker JA, Pineda JR, Grange G, Bryson EA, Guillermier M, Hirsch E, Hantraye P, *et al.* (2006) *J Clin Invest* 116:1410–1424.
30. Fox JH, Barber DS, Singh B, Zucker B, Swindell MK, Norflus F, Buzescu R, Chopra R, Ferrante RJ, Kazantsev A, *et al.* (2004) *J Neurochem* 91:413–422.
31. Karpuj MV, Becher MW, Springer JE, Chabas D, Youssef S, Pedotti R, Mitchell D, Steinman L (2002) *Nat Med* 8:143–149.
32. Borrell-Pages M, Canals JM, Cordelieres FP, Parker JA, Pineda JR, Grange G, Bryson EA, Guillermier M, Hirsch E, Hantraye P, *et al.* (2006) *J Clin Invest* 116:1410–1424.
33. Blackburn ML, Chansky HA, Zielinska-Kwiatkowska A, Matsui Y, Yang L (2003) *Biochim Biophys Acta* 1629:8–14.
34. Vaute O, Nicolas E, Vandel L, Trouche D (2002) *Nucleic Acids Res* 30:475–481.
35. Vonsattel JP, Myers RH, Stevens TJ, Ferrante RJ, Bird ED, Richardson EP, Jr (1985) *J Neuropathol Exp Neurol* 44:559–577.
36. Ferrante KL, Shefner J, Zhang H, Betensky R, O'Brien M, Yu H, Fantasia M, Taft J, Beal MF, Traynor B (2005) *Neurology* 65:1834–1836.
37. Ryu H, Ferrante R J (2005) *Exp Opin Emerg Drugs* 10:345–363.
38. Coles R, Caswell R, Rubinsztein DC (1998) *Hum Mol Genet* 7:791–800.
39. Ryu H, Lee J, Zaman K, Kubilis J, Ferrante RJ, Ross BD, Neve R, Ratan RR (2003) *J Neurosci* 23:3597–3606.